Regulation of Calcium-Permeable TRPV2 Channel by Insulin in Pancreatic β-Cells

Etsuko Hisanaga,[1,2] Masahiro Nagasawa,[1] Kohjiro Ueki,[1,3] Rohit N. Kulkarni,[4] Masatomo Mori,[2] and Itaru Kojima[1]

OBJECTIVE—Calcium-permeable cation channel TRPV2 is expressed in pancreatic β-cells. We investigated regulation and function of TRPV2 in β-cells.

RESEARCH DESIGN AND METHODS—Translocation of TRPV2 was assessed in MIN6 cells and cultured mouse β-cells by transfecting TRPV2 fused to green fluorescent protein or TRPV2 containing c-Myc tag in the extracellular domain. Calcium entry was assessed by monitoring fura-2 fluorescence.

RESULTS—In MIN6 cells, TRPV2 was observed mainly in cytoplasm in an unstimulated condition. Addition of exogenous insulin induced translocation and insertion of TRPV2 to the plasma membrane. Consistent with these observations, insulin increased calcium entry, which was inhibited by tranilast, an inhibitor of TRPV2, or by knockdown of TRPV2 using shRNA. A high concentration of glucose also induced translocation of TRPV2, which was blocked by nefedipine, diazoxide, and somatostatin, agents blocking glucose-induced insulin secretion. Knockdown of the insulin receptor attenuated insulin-induced translocation of TRPV2. Similarly, the effect of insulin on TRPV2 translocation was not observed in a β-cell line derived from islets obtained from a β-cell–specific insulin receptor knockout mouse. Knockdown of TRPV2 or addition of tranilast significantly inhibited insulin secretion induced by a high concentration of glucose. Likewise, cell growth induced by serum and glucose was inhibited by tranilast or by knockdown of TRPV2. Finally, insulin-induced translocation of TRPV2 was observed in cultured mouse β-cells, and knockdown of TRPV2 reduced insulin secretion induced by glucose.

CONCLUSIONS—TRPV2 is regulated by insulin and is involved in the autocrine action of this hormone on β-cells. ***Diabetes* 58: 174–184, 2009**

Insulin elicits pleiotropic actions in a variety of target cells and plays a pivotal role in regulating nutrient metabolism. Recent studies have revealed that the insulin signal is necessary to maintain the normal function of pancreatic β-cells. Thus, deletion of the insulin receptor (IR) in β-cells impairs insulin secretion and results in glucose intolerance (1). In β-cells of βIRKO mice, glucose-induced insulin secretion is reduced, which is accompanied by reduction of the expression of GLUT2 and glucokinase (1). However, insulin secretion induced by glyceraldehyde and KCl is also reduced in islets obtained from a βIRKO mouse (2), which cannot be explained simply by reduction of GLUT2 and/or glucokinase expression. Because addition of anti-insulin antibody immediately reduces insulin secretion from islets (3), it is likely that insulin modifies a molecule(s) involved in insulin secretion by a nongenomic mechanism. In accordance with these observations, knockdown of IR attenuates glucose-induced insulin secretion in MIN6 cells (4). In addition, postnatal β-cell growth is impaired in βIRKO mice. Consequently, the mechanism by which insulin maintains β-cell function is not totally known at present. It is thought that there must be a target molecule(s) of insulin that regulates secretion and possibly growth of β-cells.

Transient receptor potential (TRP) (5) is a calcium-permeable channel expressed in *Drosophila*. A large number of mammalian homologues have been identified, and they regulate various cellular functions (6,7). Among them, calcium-permeable cation channels resembling the vanilloid receptor channel (TRPV1) (8) have common features and now are classified as members of the TRPV subfamily (9). The TRPV subfamily consists of six members, which function as cellular sensors responding to changes in the temperature, osmolarity, and mechanical stresses, and they are also regulated by various ligands (9).

TRPV2 is regulated by heat, growth factors, and other ligands (10–13). An intriguing feature of TRPV2 is that its intracellular localization is changed by various stimulations. For example, IGF-I induces translocation of TRPV2 from an intracellular compartment to the plasma membrane (11). Regarding its expression, TRPV2 is abundantly expressed in neurons, neuroendocrine cells in the gastrointestinal tract, and blood cells such as macrophages (14). In the pancreas, TRPV2 is expressed in β-cells and ductal cells. In this regard, we previously reported that TRPV2 is expressed in an insulinoma cell line MIN6 (11). When MIN6 cells are cultured in a serum-free condition, immunoreactivity of TRPV2 is localized in an intracellular compartment. Addition of serum induces translocation of TRPV2 to the plasma membrane (11).

In the present study, we further investigated regulation of TRPV2 in β-cells. Because these cells secrete insulin, and the mode of action of insulin resembles that of IGF-I, special attention was paid to the effect of insulin and insulin secretagogues on the localization of TRPV2. The results indicate that TRPV2 is regulated by insulin in an autocrine manner in β-cells. TRPV2 functions as an insulin-mediated regulator of calcium entry.

From the [1]Institute for Molecular and Cellular Regulation, Gunma University, Maebashi, Japan; the [2]Department of Medicine and Molecular Science, Gunma University Graduate School of Medicine, Maebashi, Japan; the [3]Department of Metabolic Diseases, Graduate School of Medicine, University of Tokyo, Tokyo, Japan; and the [4]Department of Medicine, Joslin Diabetic Center, Harvard Medical School, Boston, Massachusetts.

Corresponding author: Itaru Kojima, ikojima@showa.gunma-u.ac.jp.

Received 6 June 2008 and accepted 10 October 2008.

Published ahead of print at http://diabetes.diabetesjournals.org on 4 November 2008. DOI: 10.2337/db08-0862.

RESEARCH DESIGN AND METHODS

Materials. Bovine insulin, diazoxide, and ruthenium red (RuR) were purchased from Sigma Chemical (St. Louis, MO). 1,2-Bis (*o*-aminophenoxy)ethane-N, N, N′, N′-tetraacetic acid tetra(acetoxymethyl) ester (BAPTA-AM) and Dulbecco's modified Eagle's medium (DMEM) were obtained from Invitrogen (Carlsbad, CA). D-(−)-Mannitol was obtained from Wako Pure Chemical Industries (Osaka, Japan). Anti-Myc Tag (clone 9E10) monoclonal IgG was obtained from Upstate (Lake Placid, NY) and anti-TRPV2 antibody was from Biomol (Plymouth Meeting, PA). LY294002 was from Merck Calbiochem (Darmstadt, Germany). Somatostatin was purchased from the Peptide Institute (Osaka, Japan). [^{3}H]Thymidine was obtained from Amersham (Backs, U.K.), and fura-2 was from Dojindo (Kumamoto, Japan). Tranilast was provided by Kissei Pharmaceuticals (Matsumoto, Japan).

Cell culture. Mouse MIN6, βIRKO, and control βWT cells (1,15) were maintained in DMEM containing 25 mmol/l glucose and 15% fetal bovine serum (FBS) at 37°C under a humidified atmosphere containing 5% CO_2. CHO cells were cultured in DMEM containing 10% FBS.

Islets were isolated from Balb/c mice by pancreatic duct injection of collagenase solution followed by digestion (16). Isolated islets were dispersed by incubation in 0.5 mmol/l EDTA-containing Hank's balanced salt solution (HBSS). Isolated cells were cultivated in RPMI medium containing 10% FBS. β-Cells were identified by staining with anti-insulin antibody.

Extraction of RNA and RT-PCR. Total RNA was prepared using TRIzol reagent (Invitrogen). cDNA was synthesized from total RNA using the superscript first-strand synthesis system (Invitrogen) and primed with appropriate gene-specific primers. The synthesized cDNA was added to the PCR mixture containing platinum pfx DNA polymerase (Invitrogen) in the presence of 5′ and 3′ gene-specific primers (11). Quantitative PCR was conducted in a 20-μl reaction mixture containing SYBR Premix EX Tag (Takara Bio, Tokyo, Japan) using an ABI PRISM 7500 sequence detection system (Applied Biosystem). The oligonucleotide primers for mouse IR were purchased from Takara Bio. Primers for glyceraldehyde 3-phosphate dehydrogenase (GAPDH) and mouse TRPV2 were 5′-TGC CAC TCA GAA GAC TGT GG-3′, 5′-TTC AGC TCT GGG ATG ACC TT-3′, 5′-TAC GGT CCT GCT CGA GTG TC-3′, and 5′-TGG CTC TAA AAC CAC CAT GC-3′. Reaction mixtures were incubated for an initial denaturation at 95°C for 10 s, followed by 35 PCR cycles. Each cycle consisted of 95°C for 5 s and 60°C for 34 s. The expression level of each mRNA relative to that of GAPDH was calculated using a standard curve.

Preparation of recombinant adenovirus. The hTRPV2-flag-EGFP, hTRPV2-flag-RFP, and hTRPV2-flag-EGFP-c-myc were prepared as described previously (12). To prepare adenovirus vector, we ligated hTRPV2-flag-EGF/RFP into the Entry Vector (Invitrogen) according to the manufacturer's instructions. Because the adenoviral expression of GFP was observed at >95% at a multiplicity of infection (MOI) of 20, we infected recombinant adenovirus at 20 MOI, unless otherwise stated.

Construction of short-hairpin RNA expression. Three short-hairpin oligonucleotides and complementary strands were designed to specifically target mouse IR, and six oligonucleotides were designed to specially target mouse TRPV2. The BLOCK-iT U6 RNAi Entry Vector Kit (Invitrogen) was used for shRNA construction. To generate the recombinant adenovirus vectors expressing shRNAs for mouse IR (Ad-shIR) and mouse TRPV2 (Ad-shTRPV2), selected pENTER/U6-shRNA plasmids were recombined into the Gateway-based pAd-BLOCK-iT DEST vector (Invitrogen), according to the manufacturer's instructions. As a negative control, adenovirus expressing shRNA against LacZ (Ad-shLacZ) was generated. The sequences of effective IR-shRNA and TRPV2-shRNA are shown below. Mouse IR-shRNA: top: 5′caccGCAAGCTCTTCTTCCATTACAcgaaTGTAATGGAAGAAGAGCTTGC, bottom: 5′aaaaaGCAAGCTCTTCTTCCATTACAttcgTGTAATGGAAGAAGAGCTTGC; Mouse TRPV2-shRNA 1: top: 5′caccGCTGGCTGAACCTGCTTTATTcgaaAATAAAGCAGGTTCAGCCAGC, bottom: 5′aaaaaGCTGGCTGAACCTGCTTTATTttcgAATAAAGCAGGTTCAGCCAGC.

Detection of TRPV2 incorporated into the plasma membrane. To measure TRPV2 incorporated in the plasma membrane, cells were transfected with adenovirus vector containing c-myc–tagged TRPV2. Cells were seeded on a noncoated glass coverslip at a density of 2×10^5/ml and incubated with Krebs-Ringer bicarbonate buffer (KRB). For BAPTA loading, cells were incubated with 10 μmol/l BAPTA-AM in Ca^{2+}-free KRB containing 2.5 mmol/l glucose for 20 min before insulin stimulation. For immunostaining, cells were not permeabilized, and c-myc epitope exposed outside was detected by using anti–c-myc antibody (1:400). Diaminobenzidine was used as a chromogen. Quantification of the signal was done by using the National Institutes of Health image.

Transfection of cells and measurement of translocation of TRPV2. Cells were transfected with TRPV2-EGFP or c-myc–tagged TRPV2. After 24 h incubation, cells were rinsed three times every hour in KRB buffer containing 5 mmol/l glucose. Before stimulation, cells were preincubated in KRB buffer containing 2.5 mmol/l glucose for 30 min. To determine translocation of TRPV2, fluorescence images were recorded with an Olympus IX70 epifluorescence microscope (Olympus, Tokyo, Japan) equipped with a PXL 1400 cooled charge-coupled device camera system (Photometrics, Tucson, AR), which was operated with IP Lab Spectrum software (Signal Analysis, Vienna, VA) and a laser confocal microscope (LSM 510, Zeiss).

To assess translocation of TRPV2 semiquantitatively, we scored the expression pattern of TRPV2 on the cell surface. When >30% of the margin of the cell was positive for the TRPV2-GFP signal, the cell was considered to be translocation positive. The measurement was done independently by two researchers in a double-blinded manner.

Measurement of cytosolic free calcium concentration. Cytoplasmic free calcium concentration ($[Ca^{2+}]_c$) was monitored using fura-2. The ratio of the fluorescence intensities for each of the excitation wavelengths (F340/F380) was monitored using Aqua Cosmos (Hamamatsu Photonics, Hamamatsu, Japan) (12). In Mn^{2+}-quenching experiments, fluorescence was obtained by exciting at 360 nm. After fura-2 loading, cells were incubated in the presence or absence of insulin for 20 min in KRB buffer containing 1.25 mmol/l calcium. Then 100 μmol/l $MnCl_2$ was added to the solution, and the rate of Mn^{2+} quenching was monitored.

Measurement of [^{3}H]thymidine incorporation and cell number. Cells were seeded at a density of 2×10^5 cells/ml in a 24-well dish. Twelve hours after seeding, the cells were incubated for 4 h with serum-free DMEM containing Ad-sh-LacZ or Ad-sh-mTRPV2. Infected cells were then cultured for 40 h with 15% FBS and 25 mmol/l glucose. The cells were then incubated in DMEM containing 25 mmol/l glucose and 0.25 μCi [^{3}H]thymidine for 4 h. After incubation, cells were washed twice with 1 ml ice-cold PBS and solubilized, and radioactivity associated with trichloroacetic acid–precipitable material was counted.

For measurement of the cell number, cells were seeded at a density of 2×10^5 cells/ml in a 35-mm dish and were incubated for 4 h with serum-free DMEM containing Ad-shLacZ or Ad-shTRPV2. Infected cells were then cultured for various periods in medium containing 15% FBS and 25 mmol/l glucose, and the cell number was counted.

Insulin secretion. Insulin release was measured by batch incubation. KRB buffer supplemented with 0.1% BSA was used for the experiment. MIN6 cells were seeded at a density of 2×10^5 cells/ml in a 24-well dish and cultured for 3 days. Dispersed mouse islet cells were cultured at a destiny of 5×10^4 cell/ml in a 24-well dish. After preincubation with 1 ml KRB for 30 min, cells were then incubated in the presence of various stimulators for 60 min. The medium was centrifuged at 15,000 rpm for 5 min, and the supernatant was kept at −20°C until assay. Insulin secretion from permeabilized cells was measured as described by Jones et al. (17). Insulin was determined using an insulin radioimmunoassay kit (Eiken Chemical, Tokyo, Japan).

RESULTS

Expression of the TRPV family members in MIN6 cells. We first examined the mRNA expression of the TRPV family members in MIN6 cells. As shown in Fig. 1*A*, mRNA for TRPV2 was detected in MIN6 cells, whereas mRNA for other members of the TRPV family was not detected in this condition.

Translocation of TRPV2 induced by serum in MIN6 cells. To investigate changes in the localization of TRPV2, we transfected MIN6 cells with TRPV2-EGFP, and the GFP fluorescence was monitored. In most of the unstimulated cells, the green fluorescent protein (GFP) signal was observed diffusely in cytoplasm (Fig. 1*B*, *a*). Addition of serum-induced changes in the distribution of the GFP signal and GFP was observed in the margin of the cells. The effect of serum was observed within 15 min (Fig. 1*B*, *b*) and persisted for at least 60 min (Fig. 1*B*, *c*). To semiquantify the effect, we counted the number of cells whose GFP signal was observed in the periphery of the cell. As shown in Fig. 1*C*, addition of serum induced an approximately threefold increase in the number of cells whose GFP signal was observed in the periphery of the cells. The effect of serum was inhibited by inhibitors of phosphatidylinositol (PI) 3-kinase, LY294002 (Fig. 1*C*).

Effect of insulin on translocation of TRPV2 in MIN6 cells. The structure and function of the IGF-I receptor (18) are quite similar to those of IR, and the two receptors

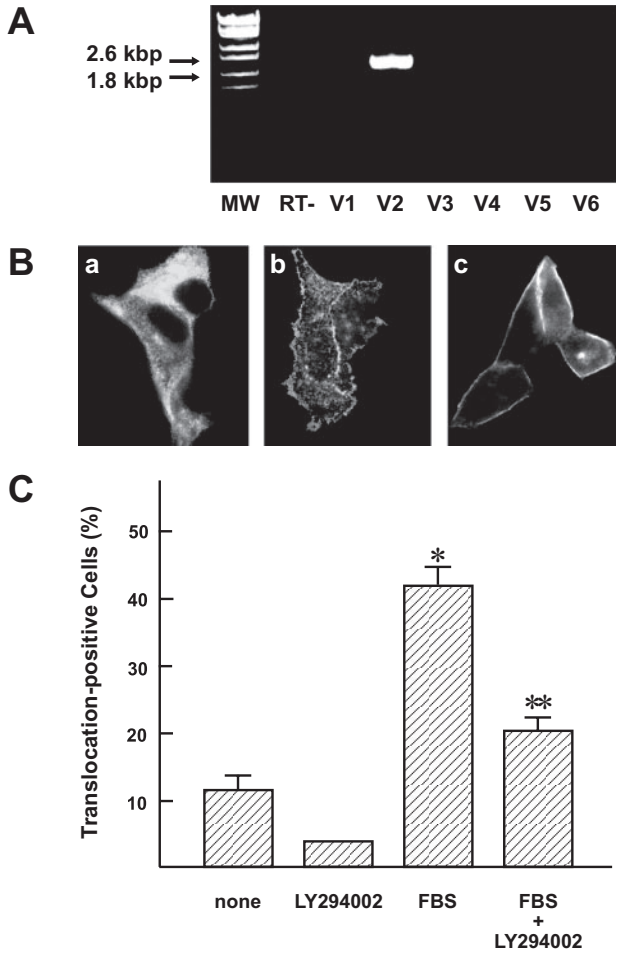

FIG. 1. Expression and translocation of TRPV2 in MIN6 cells. *A*: Expression of the TRPV family members in MIN6 cells. Expression of mRNA for various members of the TRPV family in MIN6 cells was measured by RT-PCR. Note that primers used in this study are able to detect mRNA for various members of the TRPV family (10,11). *B*: Effect of serum on localization of TRPV2. MIN6 cells were transfected with TRPV2-GFP using adenovirus vector, and the GFP fluorescence was measured. Cells were preincubated with serum-free medium for 3 h and then incubated with 15% FBS for 15 min (*b*) and 60 min (*c*). Fluorescence images before (*a*) and after stimulation (*b* and *c*) are presented. *C*: Semiquantitative analysis of the effect of serum. MIN6 cells transfected with TRPV2-GFP were incubated for 15% FBS for 30 min in the presence and absence of 50 μmol/l LY294002. The number of cells in which TRPV2 was located in the plasma membrane was counted in each condition. Data are means ± SE for five experiments, and each numbered at least 100 cells.

share a common signaling pathway (19). We therefore speculated that insulin may reproduce the IGF-I effect, and thus we addressed this possibility. Because MIN6 cells secrete insulin, endogenous insulin released from these cells may modify localization of TRPV2. We therefore monitored GFP fluorescence in cells cultured at low density. As shown in Fig. 2*A*, insulin induced translocation of TRPV2 to the plasma membrane. To confirm the effect of insulin on translocation, we determined colocalization of the TRPV2-GFP signal with a plasma membrane marker (PM) or an endoplasmic reticulum marker (ER). In the absence of insulin, the TRPV2-GFP signal was observed in cytoplasm. It was colocalized with ER (Fig. 2*B*, *a*) but not with PM (Fig. 2*B*, *b*). In the insulin-stimulated cell, the GFP signal was colocalized with PM (Fig. 2*B*, *c*).

We further examined whether TRPV2 was inserted into the plasma membrane upon stimulation by insulin. To this end, we transfected cells with c-myc–tagged TRPV2, and cell surface c-myc was stained in intact cells. Even in the absence of insulin, TRPV2 inserted into the plasma membrane was observed to some extent (Fig. 2*C*, *a*). Addition of insulin increased the amount of TRPV2 inserted into the plasma membrane (Fig. 2*C*, *b*). Quantitative analysis indicated that insulin significantly increased immunoreactivity of the c-myc tag (Fig. 2*D*). Note that immunoreactivity of the c-myc tag in unstimulated cells was reduced by loading BAPTA (Fig. 2*D*), a calcium chelator that reduced basal secretion (Fig. 2*E*). Likewise, anti-insulin antibody significantly reduced basal c-myc immunoreactivity (Fig. 2*D*). A similar experiment was done in CHO cells. In contrast to MIN6 cells, c-myc immunoreactivity was quite low in unstimulated CHO cells and was markedly increased after the stimulation by serum (Fig. 2*F*).

Figure 3*A* shows the dose-response relationship for insulin-induced translocation. This experiment was done in cells loaded with BAPTA to reduce the basal translocation of TRPV2. As depicted, the effect of insulin was detected at 500 pmol/l and was nearly maximal at 1 nmol/l. As shown in Fig. 3*B*, the effect of insulin was observed 10 min after the stimulation and became maximal within 30 min. To assess the involvement of actin filament and tubulin in insulin-induced translocation of TRPV2, we examined the effects of latrunculin A and nocodazole, respectively. As shown in Fig. 3*C*, TRPV2 translocation was inhibited by latrunculin A but not by nocodazole. Insulin-induced translocation of TRPV2 was blocked by a dominantly negative mutant of Rac. Conversely, the effect of insulin was reproduced by transfection of constitutively Rac (Supplemental Fig. 1, found in an online appendix at http://dx.doi.org/10.2337/dc08–0862). We also examined the effect of endogenous insulin on translocation of TRPV2. To this end, we stimulated the cells with a high concentration of glucose. As shown in Fig. 3*D*, 25 mmol/l glucose increased TRPV2 inserted into the plasma membrane. This was not simply due to the increase in osmolarity, since 25 mmol/l mannitol did not show any effect. The effect of glucose was inhibited by diazoxide. Similarly, somatostatin blocked glucose-induced translocation. A high concentration of potassium also induced insertion of TRPV2 into the plasma membrane (Fig. 3*E*). Note that nifedipine nearly completely blocked TRPV2 translocation induced by a high concentration of glucose and potassium. We then examined the translocation of endogenous TRPV2 using antibody recognizing the extracellular domain of TRPV2. As shown in Fig. 3*F*, insulin increased the cell surface expression of TRPV2. Likewise, high concentrations of glucose and KCl increased cell surface expression of TRPV2 (Fig. 3*G*).

We next addressed whether or not the effect of insulin was mediated by IR. We decreased the expression of IR by introducing shRNA. In cells infected with Ad-shIR, the expression of IR was markedly reduced (Fig. 4*A*). Under this condition, insulin was unable to induce translocation of c-myc–TRPV2 on the cell surface (Fig. 4*B*, *b*). In contrast, serum increased the expression of TRPV2 (Fig. 4*B*, *c*). Figure 4*C* shows quantitative analysis of the cell surface expression of c-myc in IR knocked-down cells. We also examined the effect of insulin in βIRKO cells, a cell line derived from β-cells of βIRKO mice. Insulin was unable to increase the expression of c-myc-TRPV2 in the plasma membrane (Fig. 4*D*, *b*; Fig. 4*E*, *a*), whereas serum significantly increased the cell surface expression of c-myc–TRPV2 (Fig. 4*D*, *c*; Fig. 4*E*, *a*). Note that insulin increased the expression of c-myc–TRPV2 in the plasma

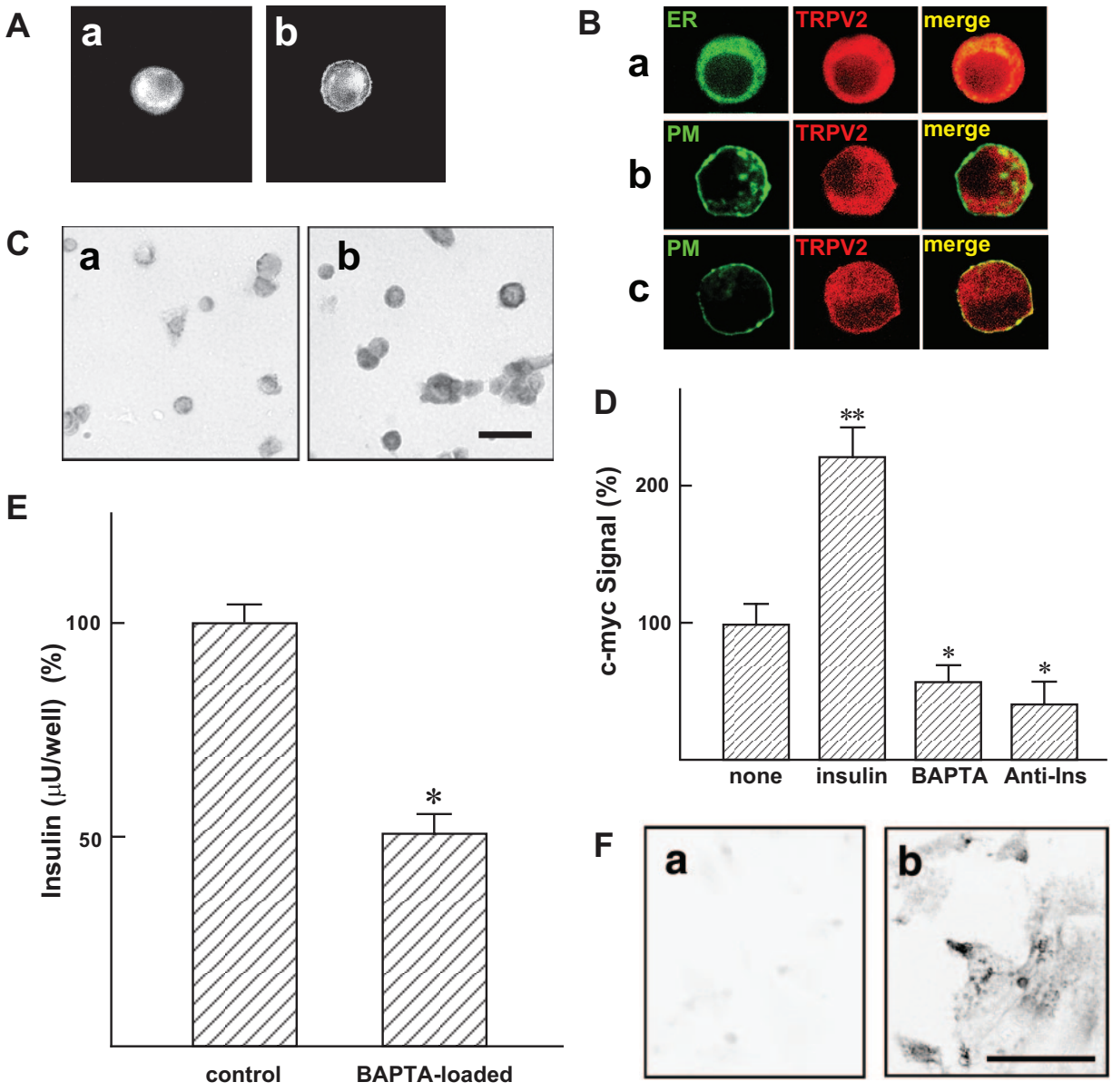

FIG. 2. Effect of insulin on translocation of TRPV2 in MIN6 cells. *A*: Effect of exogenous insulin on translocation. MIN6 cells transfected with TRPV2-GFP were preincubated with KRB buffer containing 2.7 mmol/l glucose for 1 h. They were then incubated with 10 nmol/l insulin for 30 min, and fluorescence images before (*a*) and after stimulation (*b*) are shown. *B*: Localization of TRPV2. *a*: Colocalization of TRPV2 with an ER marker. Fluorescence images were obtained in unstimulated MIN6 cells expressing TRPV2-RFP (red) and ER-YFP (green). Under a basal condition, most of the TRPV2 signals colocalized with the ER marker. *b* and *c*: Colocalization of TRPV2 with a plasma membrane marker. Fluorescence images were obtained in unstimulated (*b*) and insulin-stimulated (*c*) MIN6 cells expressing TRPV2-RFP (red) and PM-YFP (green). Under a basal condition, the TRPV2 signal was not colocalized with the PM marker, whereas some of the TRPV2 signals were colocalized with the PM marker in insulin-stimulated cells. *C*: Effect of insulin on translocation of c-myc–tagged TRPV2. MIN6 cells transfected with c-myc–tagged TRPV2 were preincubated with KRB buffer containing 2.7 mmol/l glucose for 1 h. They were then incubated for 30 min with (*b*) or without (*a*) 10 nmol/l insulin. The c-myc epitope was stained in intact cells. Bar: 20 μm. *D*: Quantification of the immunoreactivity of c-myc epitope. MIN6 cells transfected with c-myc–tagged TRPV2 were incubated for 30 min in various conditions, and cell surface expression of c-myc was quantified. Anti-Ins, anti-insulin antibody. **P* < 0.05 vs. none; ***P* < 0.01 vs. none. *E*: Effect of BAPTA loading on basal secretion of insulin. MIN6 cells loaded with or without BAPTA were incubated for 60 min in the presence of 2.7 mmol/l glucose, and insulin secretion was measured. Values are the mean ± SE for four experiments. **P* < 0.05 vs. control. *F*: Effect of serum on translocation of c-myc–tagged TRPV2 in CHO cells. CHO cells transfected with c-myc–tagged TRPV2 were incubated for 30 min with (*b*) or without (*a*) 10% serum. The c-myc epitope was stained in intact cells. Bar: 20 μm. (Please see http://dx.doi.org/10.2337/db08-0862 for a high-quality digital representation of this figure.)

membrane in the control β-cell line βWT (Fig. 4*D*, *e*; Fig. 4*E*, *b*).

Effect of insulin on calcium entry in MIN6 cells. To examine the effect of insulin on calcium entry, we monitored changes in $[Ca^{2+}]_c$ using fura-2. Fura-2–loaded cells were first incubated in calcium-free medium, and then the calcium in medium was elevated to 2 mmol/l. As shown in Fig. 5*A*, an increase in $[Ca^{2+}]_c$ was observed upon addition of calcium. A similar experiment was done in the presence of tranilast, an inhibitor of TRPV2 (20,21). A previous study indicates that 75 μmol/l tranilast markedly inhibited IGF-I–induced calcium current (21). Tranilast inhibited the elevation of $[Ca^{2+}]_c$ in response to the addition of calcium. When cells preincubated with insulin were treated in the same manner, a large increase in $[Ca^{2+}]_c$ was observed after the addition of calcium (Fig. 5*B*), indicating that insulin augmented calcium entry. Again, tranilast markedly inhibited elevation of $[Ca^{2+}]_c$. We also measured

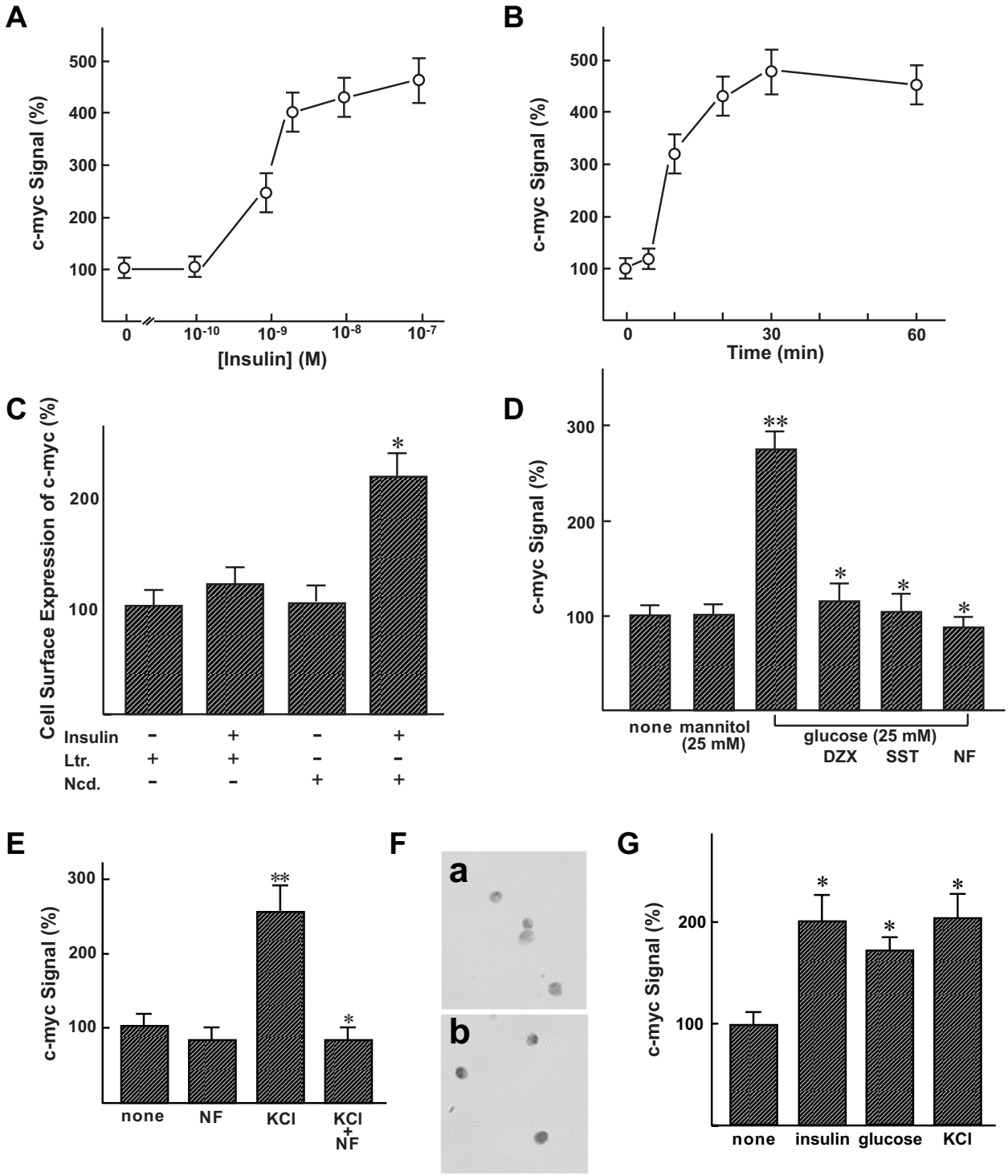

FIG. 3. Assessment of TRPV2 translocation by using c-myc–tagged TRPV2 in MIN6 cells. *A*: Dose-response relationship for the effect of insulin. MIN6 cells expressing c-myc–tagged TRPV2 were loaded with BAPTA and then incubated for 30 min with various doses of insulin, and cell surface expression of c-myc was quantified. Values are the means ± SE for three experiments. *B*: Time course of the effect of insulin. c-myc–TRPV2–expressing MIN6 cells loaded with BAPTA were incubated for various periods with 10 nmol/l insulin, and the cell surface expression of TRPV2 was measured. Values are the mean ± SE for four experiments. *C*: Effect of latrunculin A and nocodazole on translocation of TRPV2. MIN6 cells expressing c-myc–tagged TRPV2 were pretreated with 25 μmol/l latrunculin A (Ltr.) or 10 μmol/l nocodazole (Ncd.) for 30 min. Then the cells were stimulated with 10 nmol/l insulin for 30 min and the cell surface expression of TRPV2 was quantified. Values are the means ± SE for four experiments. *$P < 0.05$. *D*: Effect of glucose on translocation of TRPV2. MIN6 cells expressing c-myc–tagged TRPV2 were preincubated with KRB buffer containing 2.7 mmol/l glucose for 1 h. They were then incubated for 60 min with various agents, and cell surface expression of TRPV2 was quantified. Values are the means ± SE for four experiments. DZX, 100 μmol/l diazoxide; NF, 1 μmol/l nifedipine; SST, 10 nmol/l somatostatin. **$P < 0.05$ vs. none; *$P < 0.05$ vs. insulin. *E*: Effect of high concentration of potassium on translocation of TRPV2. MIN6 cells expressing c-myc–tagged TRPV2 were preincubated with KRB buffer containing 2.7 mmol/l glucose for 1 h. They were then incubated for 60 min with 40 mmol/l KCl in the presence and absence of 10 μmol/l nifedipine (NF), and cell surface expression of TRPV2 was quantified. Values are the means ± SE for four experiments. **$P < 0.01$ vs. none, *$P < 0.05$ vs. KCl. *F*: Translocation of endogenous TRPV2 in MIN6 cells. MIN6 cells were incubated for 20 min with (*b*) or without (*a*) 10 nmol/l insulin, and the cell surface expression of TRPV2 was measured by staining intact cells with anti-TRPV2 antibody recognizing extracellular domain. *G*: Quantification of translocation of endogenous TRPV2. MIN6 cells were incubated for 20 min with 10 nmol/l insulin, 25 mmol/l glucose, or 40 mmol/l KCl, and the cell surface expression of TRPV2 was quantified. Values are the mean ± SE for five experiments. *$P < 0.01$ vs. none.

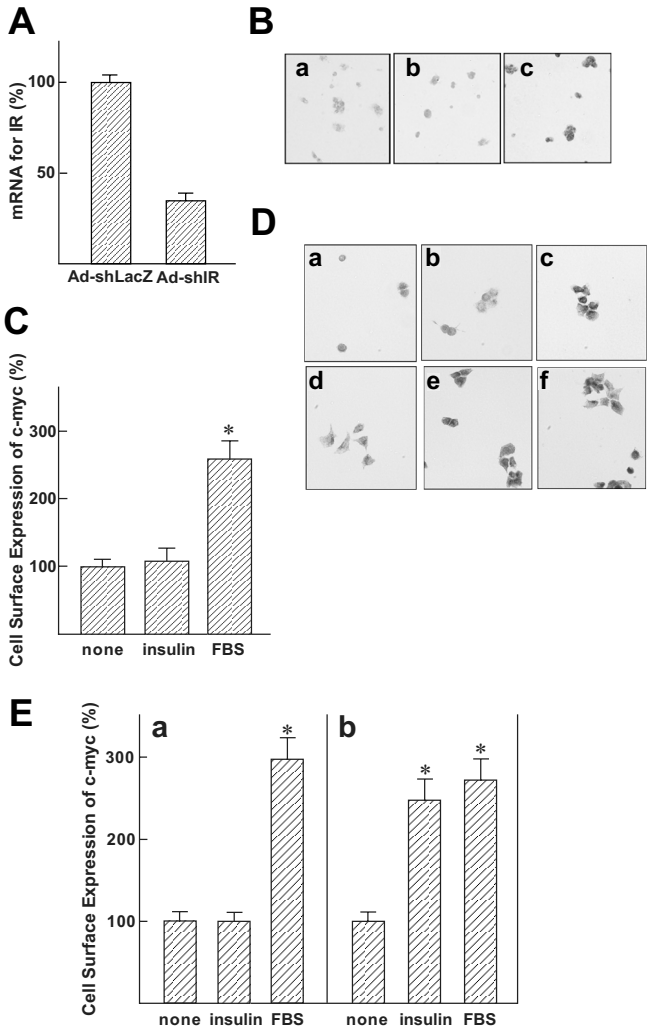

FIG. 4. Assessment of the role of the insulin receptor in insulin-induced translocation of TRPV2. *A*: Effect of shRNA on the expression of the insulin receptor. MIN6 cells were transfected with Ad-shLacZ or Ad-shIR, and the expression of IR was quantified by real-time RT-PCR. Values are the mean ± SE for four experiments. *B*: Effect of insulin in shRNA-treated cells. MIN6 cells transfected with Ad-shIR were incubated for 30 min in the absence (*a*) or presence (*b*) of 10 nmol/l insulin or 15% FBS (*c*), and cell surface expression of c-myc–TRPV2 was measured. *C*: Quantification of the results of *B*. *$P < 0.01$ vs. none. *D*: Effect of insulin and FBS on cell-surface expression of c-myc–TRPV2 in βIRKO cells. βIRKO cells (*a–c*) and control βWT cells (*d–f*) expressing c-myc–TRPV2 were incubated for 30 min in the absence (*a* and *d*) and presence (*b* and *e*) of 10 nmol/l insulin or 15% FBS (*c* and *f*), and cell surface expression of c-myc–TRPV2 was measured. *E*: Quantification of the results of *D*. *a*: βIRKO cells. *b*: Control βWT cells. *$P < 0.05$ vs. none.

calcium entry by monitoring the quenching of fura-2 by Mn^{2+}. Addition of Mn^{2+} into extracellular solution results in a time-dependent entry of Mn^{2+} through calcium-permeable channels. Once Mn^{2+} enters the cells, it reduces fura-2 fluorescence. Consequently, the rate of calcium entry is assessed by measuring the rate of quenching of fura-2 fluorescence. As shown in Fig. 5*C*, addition of $MnCl_2$ resulted in a time-dependent reduction of the fura-2 fluorescence. This was due to entry of Mn^{2+} through calcium-permeable channels. When cells were stimulated by insulin, the rate of quenching was significantly ($P < 0.01$) augmented (Fig. 5*C*). When a similar experiment was done in the presence of tranilast, basal as well as insulin-stimulated Mn^{2+} quenching was markedly reduced (Fig. 5*D*).

Effect of inhibition of TRPV2 on insulin secretion and cell proliferation in MIN6 cells. We then examined the role of TRPV2 in regulation of insulin secretion and cell growth of MIN6 cells. We first used an inhibitor of TRPV2. As shown in Fig. 6*A*, tranilast did not affect basal secretion but significantly inhibited secretion induced by glucose. Tranilast also significantly inhibited insulin secretion induced by a depolarizing concentration of potassium. To rule out the possibility that tranilast nonspecifically inhibits exocytosis of insulin, we examined whether or not tranilast affects insulin secretion induced by calcium using permeabilized cells. As shown in Fig. 6*B*, tranilast did not affect exocytosis of insulin induced by 10 μmol/l calcium in permeabilized cells. Tranilast also inhibited [^{3}H]thymidine incorporation induced by FBS and a high concentration of glucose (Fig. 6*C*) and reduced the increase in the cell number induced by FBS and a high concentration of glucose (Fig. 6*D*). Note that tranilast does not inhibit DNA synthesis induced by transfection of E2F, indicating that this compound does not affect the machinery for DNA replication (S. Nakajima, I.K., unpublished data). We also examined the role of TRPV2 by reducing its expression using shRNA. In MIN6 cells transfected with Ad-shTRPV2, expression of mRNA for TRPV2 was markedly reduced compared with that of cells transfected with Ad-shLacZ (Fig. 7*A*). Similarly, Ad-shTRPV2 markedly reduced the protein expression of TRPV2 (Fig. 7*B*). We then assessed changes in calcium entry by measuring Mn^{2+} quenching. In Ad-shTRPV2–infected cells, reduction of fura-2 fluorescence induced by addition of Mn^{2+} was small (Fig. 7*C*, *b*) compared with that in Ad-shLacZ–infected cells (Fig. 7*C*, *a*). In addition, insulin did not increase the rate of Mn^{2+} quenching in Ad-shTRPV2–infected cells (Fig. 7*C*, *b*). We then measured changes in $[Ca^{2+}]_c$ in glucose-stimulated Ad-shTRPV2–infected cells. $[Ca^{2+}]_c$ fluctuated considerably at a later time point, and we could detect significant reduction of $[Ca^{2+}]_c$ compared with that in Ad-shLacZ–infected cells (Fig. 7*D*). Likewise, $[Ca^{2+}]_c$ induced by 40 mmol/l KCl was significantly reduced at a later time point in Ad-shTRPV2–infected cells (data not shown). In this condition, glucose-induced insulin secretion was significantly inhibited in Ad-shTRPV2–infected cells (Fig. 7*F*). Likewise, insulin secretion induced by depolarizing concentration of potassium was significantly reduced. Note that the difference in insulin secretion was not due to the difference in the cell number, since the cell number was not changed in each condition. In addition, [^{3}H]thymidine incorporation induced by serum and a high concentration of glucose was significantly reduced in cells infected with Ad-shTRPV2 (Fig. 7*G*). Similarly, the increase in the cell number induced by serum was reduced in Ad-shTRPV2–infected cells compared with that of Ad-shLacZ–infected cells (Fig. 7*H*). Cell viability was not changed and cell death was not observed in Ad-shTRPV2–infected cells.

Role of TRPV2 in cultured mouse β-cells. We studied the expression of TRPV2 in mouse islets. As shown in Fig. 8*A*, TRPV2 was expressed in the core of the islet but not in α-cells. Next, we studied the effect of insulin in cultured β-cells. When cultured β-cells expressing c-myc–TRPV2 were incubated with 10 nmol/l insulin, immunoreactivity of c-myc was increased significantly after the insulin treatment (Fig. 8*B*). Figure 8*C* shows the quantitative analysis of the data. A high concentration of glucose also induced translocation of TRPV2, which was blocked by an addition of diazoxide. We then studied insulin secretion in cultured β-cells. In β-cells infected with Ad-shTRPV2,

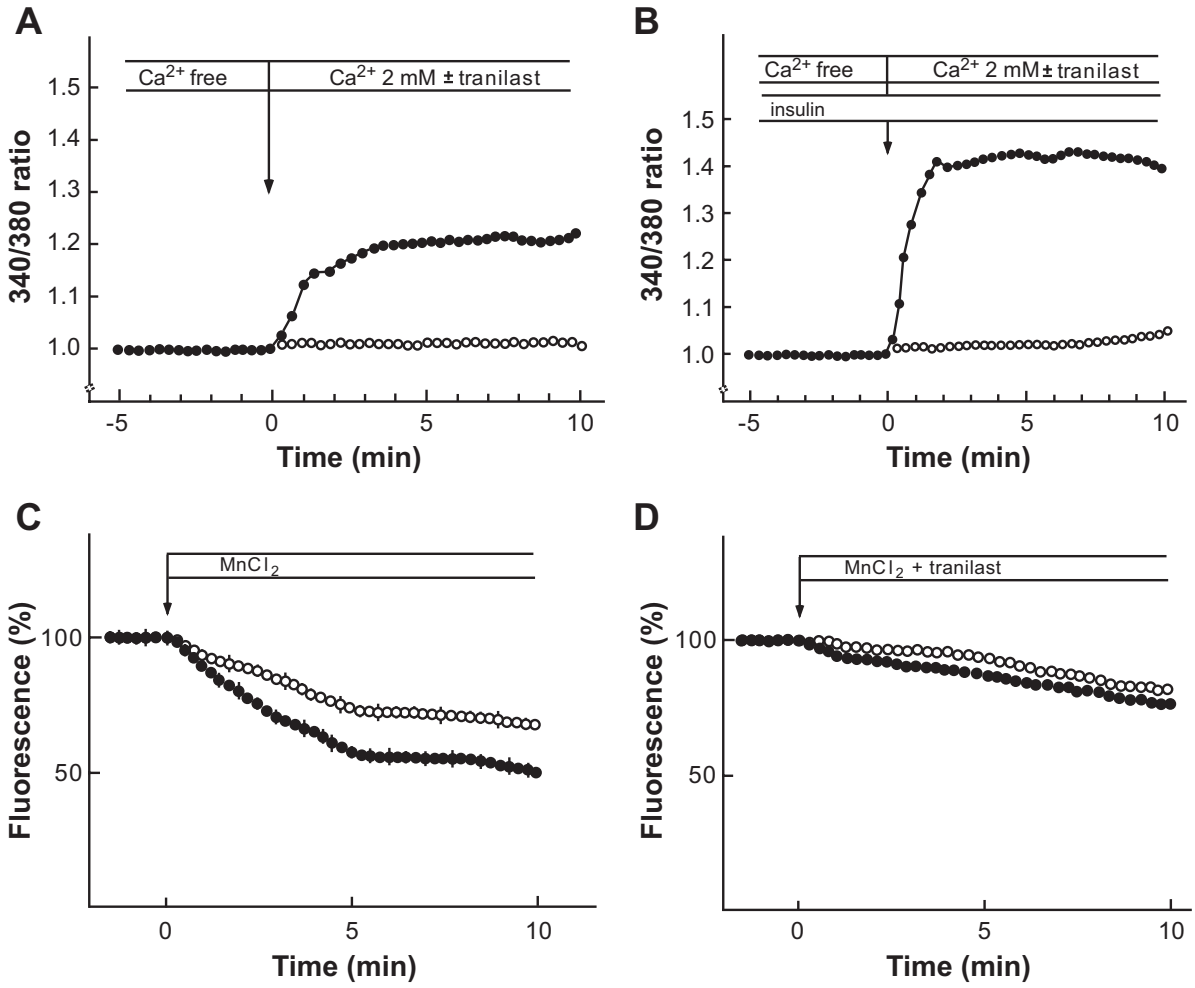

FIG. 5. Effect of insulin on calcium entry in MIN6 cells. *A* and *B*: Measurement of changes in $[Ca^{2+}]_c$. Fura-2–loaded MIN6 cells were incubated for 30 min in calcium-free KRB in the presence (*B*) and absence (*A*) of 10 nmol/l insulin. Extracellular medium was then switched to 2 mmol/l calcium-containing KRB with (○) or without (●) 75 μmol/l tranilast as indicated, and changes in the $[Ca^{2+}]_c$ were monitored. The results are representative of at least 10 experiments. *C*: Measurement of calcium entry by monitoring Mn^{2+} quenching. Fura-2–loaded MIN6 cells were incubated for 20 min in the presence (●) or absence (○) of 10 nmol/l insulin. $MnCl_2$ (0.1 mmol/l) was then added, and changes in the fluorescence were monitored. Values are the mean ± SE for five determinations and representative of five experiments with similar results. *D*: Effect of tranilast on Mn^{2+} quenching. Experiments were done as shown in *C* except that 75 μmol/l tranilast was added together with $MnCl_2$.

insulin secretion induced by a high concentration of glucose was significantly reduced. Similarly, insulin secretion induced by potassium was significantly reduced in Ad-shTRPV2–infected cells (Fig. 8*D*).

DISCUSSION

In this study, we showed that insulin induced translocation and insertion of TRPV2 into the plasma membrane. Consistent with these observations, calcium entry as monitored by fura-2 fluorescence was elevated in cells pretreated with insulin, which was inhibited by an inhibitor of TRPV2 and knockdown of TRPV2. Collectively, exogenous insulin induces translocation of TRPV2 to the plasma membrane and augments calcium entry. In our experimental condition, translocation of TRPV2 was observed to some extent under basal conditions. This is in sharp contrast to CHO cells and macrophages (12), where the amount of TRPV2 in the plasma membrane is very low in an unstimulated condition. This difference may be explained by the basal secretion of insulin, since the basal level of translocation is reduced by loading BAPTA, which reduces basal secretion, and by anti-insulin antibody. These observations imply that translocation of TRPV2 induced by basal release of insulin may contribute to basal calcium entry. Furthermore, translocation of TRPV2 was induced by insulin secretagogues including a high concentration of glucose. Taken together, insulin released from β-cells further augments calcium entry by recruiting TRPV2 to the plasma membrane. Given that calcium is a critical regulator of insulin secretion, this is a feed-forward mechanism to accelerate insulin secretion. With regard to the functional significance of TRPV2, inhibition of the TRPV2 activity by tranilast or by knockdown of TRPV2 using shRNA reduces glucose-induced insulin secretion. Augmented calcium entry through TRPV2 may contribute partly to glucose-induced insulin secretion. Also, TRPV2 is involved in insulin secretion induced by other secretagogues. For example, potassium-induced secretion is also inhibited partly by inhibiting TRPV2. Presumably, insulin released by depolarization of β-cells in turn recruits TRPV2 to the plasma membrane, which leads to additional calcium entry through TRPV2 and thereby enhances insulin secretion. It is known that voltage-dependent calcium channels are downregulated (so-called inactivation) rather quickly after depolarization of the plasma membrane. In contrast, the TRPV2 channel is not downregulated quickly.

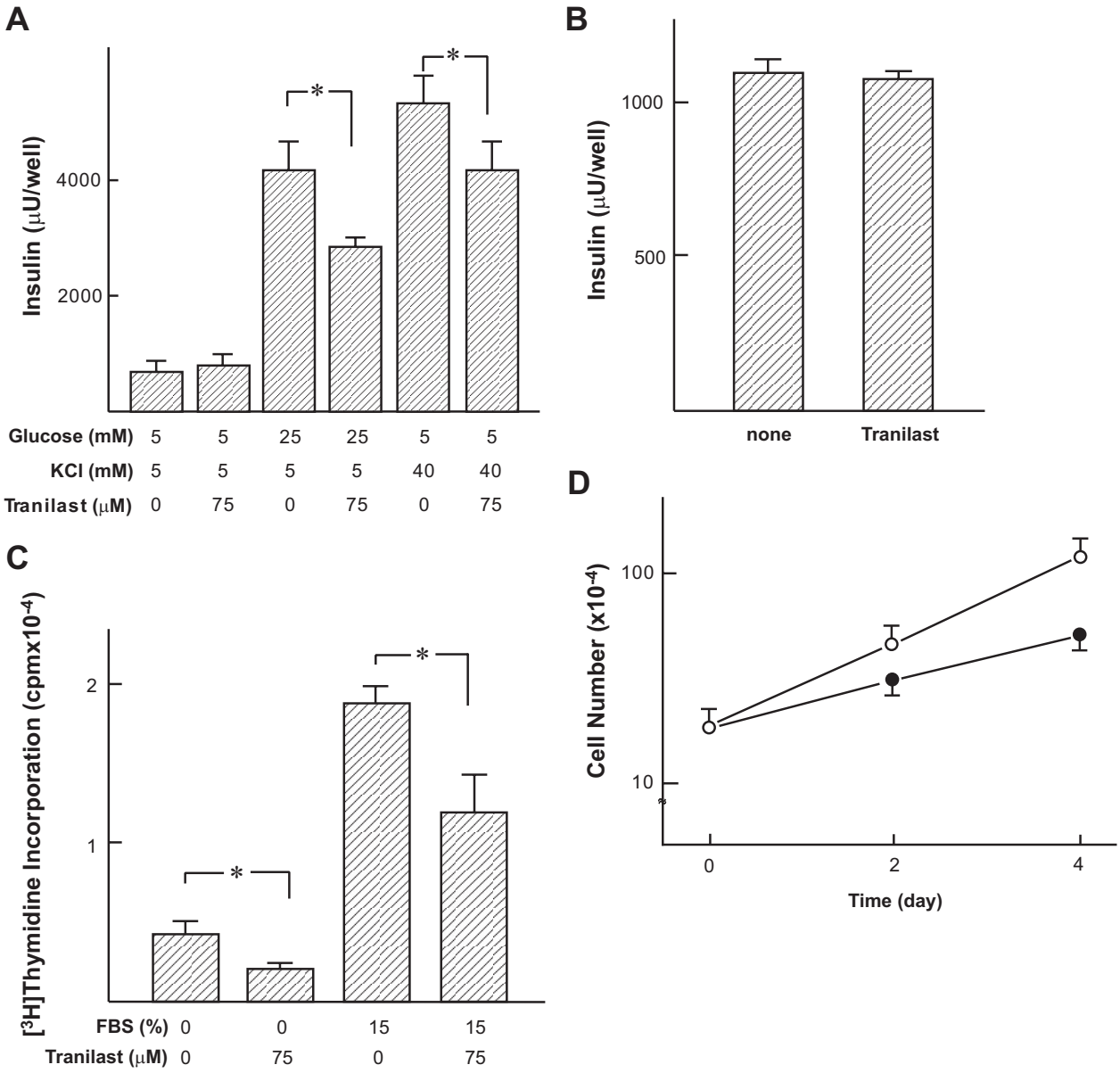

FIG. 6. Effect of tranilast on insulin secretion and proliferation in MIN6 cells. *A*: Effect of tranilast on insulin secretion. MIN6 cells were preincubated with KRB buffer containing 2.7 mmol/l glucose for 30 min. They were then stimulated with 25 mmol/l glucose or 40 mmol/l KCl for 60 min in the presence and absence of 75 μmol/l tranilast. Values are the mean ± SE for four determinations, and the results are representative of three experiments. *$P < 0.05$. *B*: Effect of tranilast on insulin secretion in permeabilized cells. Permeabilized MIN6 cells were incubated for 60 min with 10 μmol/l calcium in the presence and absence of 75 μmol/l tranilast. Insulin secretion in medium containing EGTA was subtracted. Values are the mean ± SE for four experiments. *C*: Effect of tranilast on [^{3}H]thymidine incorporation. MIN6 cells were incubated for 48 h with or without 15% FBS and 25 mmol/l glucose in the presence and absence of 75 μmol/l tranilast, and [^{3}H]thymidine in corporation was then measured. Values are the mean ± SE for four experiments. *$P < 0.05$. *D*: Effect of tranilast on the cell number. MIN6 cells were incubated for various periods with 15% FBS and 25 mmol/l glucose in the presence (●) and absence (○) of 75 μmol/l tranilast. Values are the mean ± SE for three experiments, and the cell number was counted. *$P < 0.05$ vs. none.

Instead, it promotes calcium entry for a relatively long period (11). Consequently, recruitment of TRPV2 by insulin may prolong calcium entry into β-cells. TRPV2 is a calcium-permeable channel and also permeates sodium as well (11). Translocation of TRPV2 thus also increases sodium entry into β-cells. This leads to depolarization of the plasma membrane and subsequent activation of the voltage-dependent calcium channels. Recently, it was reported that TRPM2 and TRPM4 are involved in glucose-induced insulin secretion in pancreatic β-cells (22,23). TRPM2 and TRPM4 permeate calcium and/or sodium, which leads to depolarization of the plasma membrane and activation of the voltage-gated calcium channel. In addition to the well-known role of the voltage-gated calcium channels, members of the TRP channel family may contribute to the stimulus-secretion coupling in β-cells.

The autocrine effect of secreted insulin on β-cell function has been a matter of debate. Both positive and negative feedback regulations have been postulated, and there have been many reports supporting these ideas (rev. in 24). In this regard, a study using β-cell–specific knockout of the IR gene demonstrated that blocking of the insulin action in β-cells impairs glucose-induced insulin secretion and also reduces the β-cell mass in adults (1). The present results suggest that TRPV2 is one of the target molecules of insulin and may participate at least partly in the trophic action of this hormone in β-cells. Inhibition of the TRPV2 reduces insulin secretory response and DNA

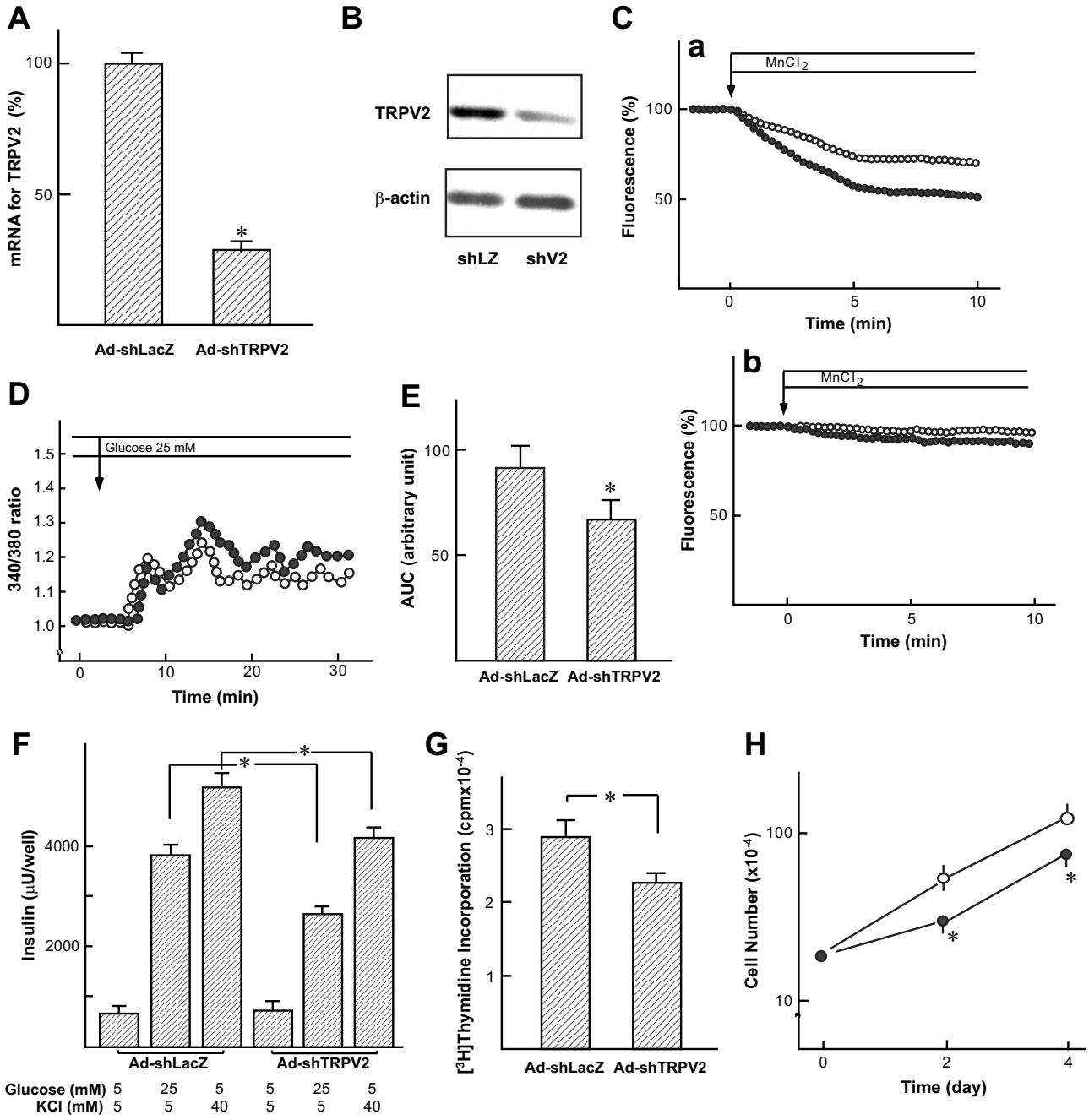

FIG. 7. Effect of shRNA for TRPV2 on insulin secretion and proliferation in MIN6 cells. *A*: Effect of Ad-shTRPV2 on the expression of mRNA for TRPV2. MIN6 cells were transfected with Ad-shLacZ or Ad-shTRPV2, and the expression of mRNA for TRPV2 was measured by real-time RT-PCR. Values are the mean ± SE for four experiments. *$P < 0.05$ vs. Ad-shLacZ. *B*: Effect of Ad-shTRPV2 on the protein expression of TRPV2. MIN6 cells were transfected with Ad-shLacZ (shLZ) or Ad-shTRPV2 (shV2). Expression of TRPV2 was measured by immunoblotting. *C*: Effect of knockdown of TRPV2 on calcium entry. MIN6 cells were transfected with Ad-shLacZ (*a*) or Ad-shTRPV2 (*b*). Calcium entry was assessed by measuring Mn^{2+} quenching in the presence (●) and absence (○) of 10 nmol/l insulin. *D*: Effect of knockdown of TRPV2 on glucose-induced changes in $[Ca^{2+}]_c$. MIN6 cells infected with Ad-shTRPV2 (○) or Ad-shLacZ (●) were stimulated with 25 mmol/l glucose, and $[Ca^{2+}]_c$ was monitored. *E*: Effect of knockdown of TRPV2 on glucose-induced elevation of $[Ca^{2+}]_c$. Experiments were performed as shown in Fig. 7*D*, and area under the curve (AUC) was calculated. Values are the mean ± SE for five experiments. *$P < 0.05$ vs. shLacZ. *F*: Effect of shRNA for TRPV2 on insulin secretion. MIN6 cells were infected with Ad-shLacZ or Ad-shTRPV2. Infected cells were preincubated with KRB buffer containing 2.7 mmol/l glucose for 30 min. They were then incubated for 60 min with 25 mmol/l glucose or 40 mmol/l KCl, and secreted insulin was measured. Values are the mean ± SE for four determinations and are representative of three experiments. *$P < 0.05$. *G*: Effect of shRNA for TRPV2 on [^{3}H]thymidine incorporation. MIN6 cells were infected with Ad-shLacZ or Ad-shTRPV2. Infected cells were further incubated for 48 h with 15% FBS and 25 mmol/l glucose, and [^{3}H]thymidine incorporation between 44 and 48 h was measured. Values are the mean ± SE for four experiments. *$P < 0.05$. *H*: Effect of shRNA for TRPV2 on the cell number. MIN6 cells were infected with Ad-shLacZ (○) or Ad-shTRPV2 (●) and incubated for indicated period with 15% FBS and 25 mmol/l glucose. The number of cells was counted. Values are the mean ± SE for four experiments. *$P < 0.05$ vs. Ad-shLacZ–treated cells.

synthesis in these cells. Given that stimulation of calcium entry is a prerequisite for cell-cycle progression induced by growth factors (25,26), it is likely that TRPV2 plays a role in insulin-induced proliferation. Taken together, TRPV2 functions as one of the molecular targets of the insulin action and modulates calcium entry.

We studied the role of TRPV2 in MIN6 cells and dispersed β-cells. It is uncertain at present whether or not

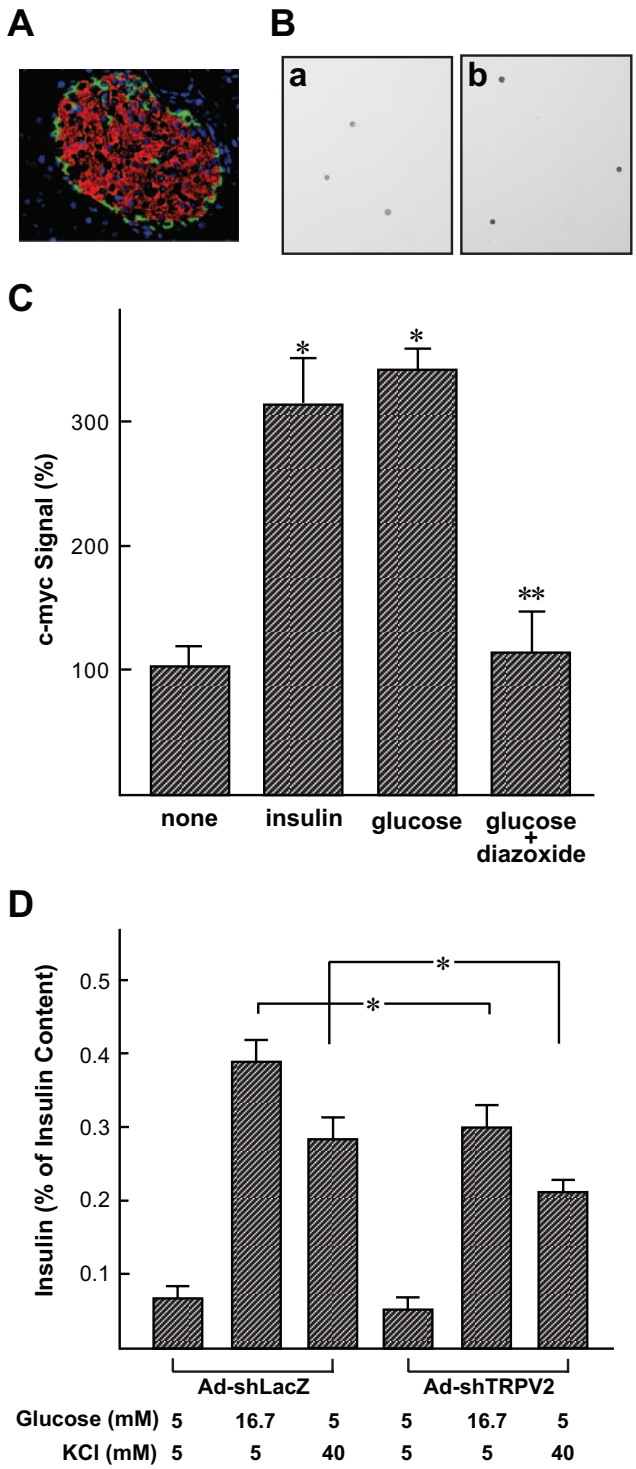

FIG. 8. Effect of insulin on TRPV2 translocation in mouse β-cells. *A*: Expression of TRPV2 in mouse islet. Mouse pancreatic section was stained with anti-TRPV2 (red) and anti-glucose (green) antibodies. Nuclei were stained with DAPI (blue). *B*: Effect of insulin on the cell surface expression of c-myc epitope in cultured β-cells. c-myc–TRPV2–expressing cultured β-cells were incubated with (*b*) or without (*a*) 10 nmol/l insulin for 30 min, and intact cells were stained with anti–c-myc antibody. *C*: Quantification of the effect of insulin and glucose on TRPV2 translocation. c-myc–TRPV2–expressing β-cells were incubated for 60 min with various agents, and cell surface c-myc TRPV2 was quantified. Values are the mean ± SE for four experiments. *$P < 0.05$ vs. none. **$P < 0.05$ vs. glucose. *D*: Effect of Ad-shTRPV2 on insulin secretion from cultured β-cells. Cultured β-cells were infected with Ad-shLacZ or Ad-shTRPV2. Cells were preincubated for 30 min with KRB buffer containing 2.7 mmol/l glucose. They were then incubated for 1 h with 16.7 mmol/l glucose or 40 mmol/l KCl, and insulin secretion was quantified. Data are means ± SE for four experiments. *$P < 0.05$. (Please see http://dx.doi.org/10.2337/db08-0862 for a high-quality digital representation of this figure.)

insulin secreted from β-cells actually controls translocation of TRPV2 in islet β-cells in vivo. It is possible that basal secretion of insulin induces translocation of TRPV2 and TRPV2 is always operative in the plasma membrane. It is also possible that growth factors in plasma, for example IGF-I, induces translocation and TRPV2 is always functional. If so, insulin secretagogues do not regulate TRPV2 translocation. Instead, changes in the expression of TRPV2, if any, would alter the basal rate of calcium entry. Further studies are necessary to assess the in vivo role of TRPV2 in β-cells.

The present results provide for the first time evidence that calcium-permeable channel TRPV2 is a signaling molecule involved in the insulin action. In this regard, insulin is shown to recruit various types of ion channels to the plasma membrane in neuronal cells (27–29). TRPV2 is one of the channel molecules regulated by insulin. Many issues are still unsolved. For example, it is not known whether insulin directly modifies gating of the TRPV2 in addition to induction of translocation. Further studies are necessary to elucidate the role of TRPV2 in the insulin action.

ACKNOWLEDGMENTS

The present study was supported by a Grant-in-Aid for Exploratory Research for the Ministry of Science, Education, Sports and Culture of Japan (to I.K.); the Global COE Program of Japan (to I.K.); and NIH Grant RO1 DK67536 (to R.N.K.).

No potential conflicts of interest relevant to this article were reported.

The authors are grateful to Mayumi Odagiri for secretarial assistance.

REFERENCES

1. Kulkarni RN, Bruning JC, Winnay JN, Postic C, Magnuson MA, Kahn CR: Tissue-specific knockout of the insulin receptor in pancreatic β cells creates an insulin secretory defect similar to that in type 2 diabetes. *Cell* 96:329–339, 1999
2. Otani K, Kulkarni RN, Baldwin AC, Krutzfeldt J, Ueki K, Stoffel M, Kahn CR, Polonski KS: Reduced β-cell mass and altered glucose sensing impair insulin-secretory function in βIRKO mice. *Am J Physiol* 286:E41–E49, 2004
3. Strivastava S, Goren HJ: Insulin constitutively secreted by β-cells is necessary for glucose-stimulated insulin secretion. *Diabetes* 52:2049–2056, 2003
4. Silva Xavier G, Qian Q, Cullen PJ, Rutter GA: Distinct roles for insulin and insulin-like growth factor receptors in pancreatic β-cell glucose sensing revealed by RNA silencing. *Biochem J* 377:149–158, 2004
5. Montell CK, Jones K, Hafen E, Rubin G: Rescue of the Drosophila phototransduction mutation *trp* by germline transformation. *Science* 230: 1040–1043, 1985
6. Clapham DE: TRP channels as cellular sensors. *Nature* 426:517–524, 2003
7. Ramsey IS, Delling M, Clapham DE: An introduction to TRP channels. *Ann Rev Physiol* 68:619–647, 2006
8. Caterina MJ, Schumacher MA, Tominaga M, Rosen TA, Levine JD, Julius D: The capsaicin receptor: a heat-activated ion channel in the pain pathway. *Nature* 389:816–824, 1997
9. Gunthorpe MJ, Benham CD, Randall A, Davis JB: The diversity in the vanilloid (TRPV) receptor family of ion channels. *Trends Pharmacol Sci* 23:183–191, 2002
10. Boels K, Glassmeier G, Herrmann D, Riedel B, Hampe W, Kojima I, Schwartz JR, Schaller JR: The neuropeptide head activator induces activation and translocation of the growth-factor-regulated Ca^{2+}-permeable channel GRC. *J Cell Sci* 114:3599–3606, 2001
11. Kanzaki M, Zhang YQ, Mashima H, Li L, Shibata H, Kojima I: Translocation of a calcium-permeable cation channel by insulin-like growth factor-I. *Nat Cell Biol* 1:165–170, 1999
12. Nagasawa M, Nakagawa Y, Tanaka S, Kojima I: Chemotactic factor formyl-Met-Len-Phe induces translocation of TRPV2 in macrophage. *J Cell Physiol* 210:692–702, 2007

13. Stokes AJ, Shimoda LMN, Koblan-Huberson M, Adra CN, Turner H: A TRPV2-PKA signaling module for transduction of physical stimuli in mast cells. *J Exp Med* 200:137–147, 2004
14. Kowase T, Nakazato Y, Kuro-o Y, Morikawa A, Kojima I: Immunohistochemical localization of growth factor-regulated channel (GRC) in human tissues. *Endocrine J* 49:349–355, 2002
15. Kulkarni RN, Winnay JN, Daniels M, Bruning JC, Fleir SN, Hanahan D, Kahn CR: Altered function of insulin receptor substrate-deficient mouse islets and cultured β-cell line. *J Clin Invest* 104:R69–R75, 1999
16. Goto M, Maki T, Koizumi T, Satomi S Manaco AP: A improved method for isolation of mouse pancreatic islet. *Transplantation* 40:437–438, 1985
17. Jones PM, Fyles JM, Howell SL: Regulation of insulin secretion by cAMP in rat islets of Langerhans permeabilized by high-voltage discharge. *FEBS Lett* 205:205–209, 1986
18. Ullrich A, Gray A, Tam AW, Yang-Feng T, Tsubokawa M, Collins C, Henzel W, Bon TL, Kathuria S, Chen E, Jacobs S, Francke U, Ramachandran J, Fujita-Yamaguchi Y: Insulin-like growth factor-I receptor primary structure. *EMBO J* 5:2503–2512, 1986
19. Czech M: Signal transmission by the insulin-like growth factors. *Cell* 59:235–238, 1989
20. Nie L, Ohnishi H, Doi I, Shibata H, Kojima I: Inhibition of proliferation of MCF-7 breast cancer cells by a blocker of calcium-permeable cation channel. *Cell Calcium* 22:75–82, 1997
21. Nie L, Kanzaki M, Shibata H, Kojima I: Activation of calcium-permeable cation channel by insulin in Chinese hamster ovary cells expressing human insulin receptors. *Endocrinology* 139:179–188, 1998
22. Cheng H, Beck A, Launay P, Gross SA, Stokes AJ, Kinet JP, Fleig A, Penner R: TRPM4 controls insulin secretion in pancreatic β cells. *Cell Calcium* 41:51–61, 2007
23. Togashi K, Hara Y, Tominaga T, Higashi K, Konishi Y, Mori Y, Tominaga M: TRPM2 activation by cyclic ADP-ribose at body temperature is involved in insulin secretion. *EMBO J* 25:1804–1815, 2006
24. Leibiger IB, Leibiger B, Berggren PO: Insulin feedback action on pancreatic β cell function. *FEBS Lett* 532:1–6, 2002
25. Lu KP, Means AR: Regulation of the cell-cycle by calcium and calmodulin. *Endocrine Rev* 14:40–58, 1993
26. Kojima I, Mogami H, Shibata H, Ogata E: Role of calcium entry and protein kinase C in the progression activity of IGF-I in Balb/c 3T3 cells. *J Biol Chem* 268:10003–10006, 1993
27. Wan Q, Xiong ZG, Man HY, Ackerley CA, Braunton J, Lu WT, Becker LE, MacDonald JF, Wang YT: Recruitment of functional GABA receptors to postsynaptic domains by insulin. *Nature* 388:686–690, 1997
28. Skeberdis VA, Lan J, Zheng X, Zukin RS, Bennett MV: Insulin promotes rapid delivery of NMDA receptors to the cell surface by exocytosis. *Proc Natl Acad Sci U S A* 98:3561–3566, 2001
29. Van Buren JJ, Bhat S, Rotello R, Pauza ME, Premkumar LS: Sensitization and translocation of TRPV1 by insulin and IGF-I. *Mol Pain* 1:17–27, 2005